Comparison of compressor control strategies for solar direct drive refrigerators

Jensen, Jonas K.; Moeller, Hendrik; Katic, Ivan; Pedersen, Per Henrik ; Markussen, Wiebke Brix

Published in:
Proceedings of the 25th IIR International Congress of Refrigeration

Link to article, DOI:
10.18462/iir.icr.2019.1086

Publication date:
2019

Document Version
Peer reviewed version

Manuscript ID: 1086
DOI: 10.18462/iir.icr.2019.1086

Comparison of compressor control strategies for solar direct drive refrigerators

Jonas K. JENSEN[(a)], Hendrik MOELLER[(C)], Ivan KATIC[(b)], Per Henrik PEDERSEN[(b)], Wiebke B. MARKUSSEN[(b)]

[(a)] Department of Mechanical Engineering, Technical University of Denmark
Kgs Lyngby, 2800
[(b)] Danish Technological Institute,
Gregersensvej 2, DK-2630 Taastrup
[(c)] Nidec Global Appliance Germany GmbH,
Flensburg, 24939, Germany, europe@mail.nidec.com

ABSTRACT

The influence of the applied compressor control strategy on the performance of a solar direct drive refrigeration system was investigated using numerical modelling and simulations. Two compressor types and three compressor control strategies where investigated. Further, four configurations where included: a 360 W and a 180 W PV panel both with and without compressor start power delivered from the PV panel. Results showed that both the choice of compressor and the applied control strategy affected the systems ability to utilize the available power from the PV panel, especially under lower irradiance conditions and when the PV panel was downsized. However, results show that if the need for compressor start power delivered by the PV panel was alleviated the size of the PV panel can be halved without significant reductions in performance.
Keywords: Solar Direct Drive, PV Panel, Control Strategy, Compressor Speed Control, Ice Bank Storage.

1. INTRODUCTION

People in rural areas of many developing countries have non or unreliable access to electricity (IEA, 2012). In such areas correct storage of temperature sensitive products such as food or more importantly medical equipment such vaccines is a significant challenge. This may affect as many as 1.3 billion people worldwide (IEA, 2012), wherefore finding good solutions for off-grid refrigerators is an important task.

Different types of absorption refrigeration systems driven by combustibles such as kerosene or gas have been developed but have been found to be unreliable and require high maintenance (McCarney et al., 2013). Alternatively solar driven systems have been developed since the 1980s first utilizing batteries to store electricity to power the system during night time. Later battery free systems or solar direct drive system have been developed as presented by Pedersen et al. (2019). McCarney et al. (2013) state that battery free solar direct drive systems are the most promising solution for off-grid vaccine storage.

Myers et al. (2017) investigate the potential for harvesting excess energy from solar direct drive refrigerators applied as medical cold chain equipment and found that significant amounts of energy could be utilized to power secondary equipment without compromising the temperature of the stored goods. This is investigated with a traditional on/off compressor control. The potential to harvest excess energy may though be reduced if more advanced compressor control strategies are applied. The present work focused on analysing the operation of a direct drive solar powered refrigeration

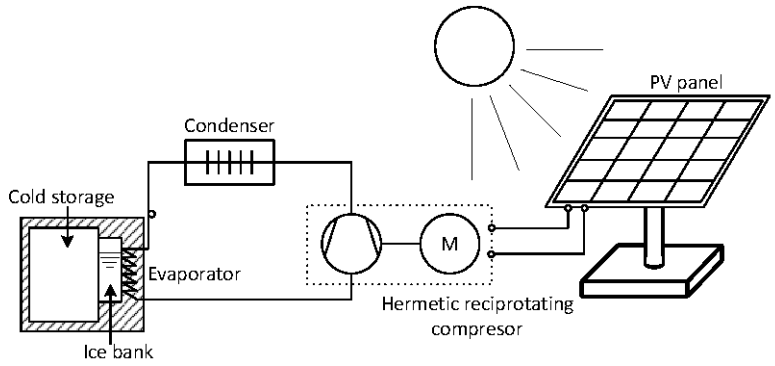

Figure 1: Principle sketch of the direct drive solar refrigeration system with ice bank storage

system with an ice bank storage under different compressor control strategies. A principle sketch of such a system may be seen in Fig. 1. As seen the refrigeration system consists of a hermetic reciprocating compressor, a finned tube condenser, a capillary tube and an evaporator placed in direct contact with an ice bank storage.

2. METHODS

In a configuration such as the one seen in Fig. 1 it is the control of the compressor speed that will ensure optimal utilization of the available power from the PV panel. Here it is important to realize that the operation of a PV panel is characterized by the voltage - current curves seen in Fig. 2 (right). Herethe solid black lines represent the voltage - current relation for a given solar irradiance. As seen for a given solar irradiance the current first shows a small decrease with increased voltage up to, in this case 25 V, where after it will experience a rapid decrease to a current of 0 A. Further, the greater the solar irradiance the higher the current will be for the same voltage.
Realizing that the power extracted from the PV panel is the product of the voltage and current results in the dashed blue lines. These naturally assume values of 0 W when either the voltage or current are 0. Further, it may be seen that for each solar irradiance there is a peak power point and that this point occurs at approximately the same voltage. Finally, it is seen that the higher the solar irradiance the higher the peak power.
If the system driven by the PV panel, in this case the compressor, tries to draw more power from the panel than the peak power at the given irradiance, the PV panel will experience was is called a collapse. A collapse results in no power being delivered and consequently that the system is turned off. If the compressor is run to fast there is thus a risk that it will collapse the PV panel and force a shut down of the system. However, if the compressor is run to slow, the refrigeration system will not be utilizing as much of the available power.
Therefore, it is relevant to find compressor control strategies that can ensure that the system will operate as close to the peak power point as possible at the varying solar irradiance the system will experience during a day or a year. In the present work is was assumed that the PV panel was south facing and located on the northern hemisphere somewhere close to the equator. On a location such as this the duration of which sunlight will reach the PV panel is roughly 8 hours per day with the peak irradiance in the middle of this period and a symmetrical increase and decrease around the peak.

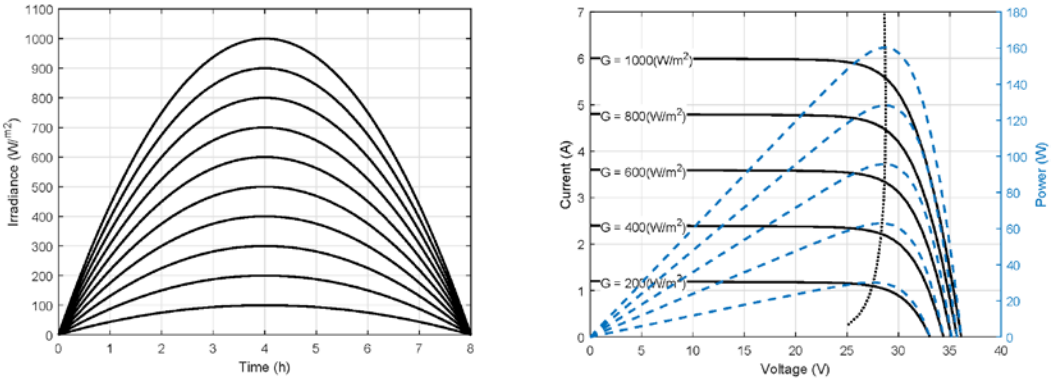

Figure 2: Daily solar profile and principle sketch of the operating characteristics of a PV panel

A sketch of the daily solar profile may be seen in Fig. 2 (left). As seen here the profile is sketched for peak irradiances from 100 Wm^{-1} to 1000 Wm^{-1}. These peak irradiance variations may resemble both seasonal variation but also cloud covers of different intensity. The present work will be limited to the smooth profiles seen in Fig. 2 and will thus not include spotted cloud covers and the rapid transients involved in these. The different compressors and compressor control strategies will be evaluated at the different range of solar profiles seen in Fig. 2. This, as it was relevant to investigate both the minimum peak irradiance needed for the system to deliver a cooling load but also the peak irradiance at which the available power from the solar panel cannot be fully utilized due to speed restriction of the compressor.
To perform this investigation numerical models where developed for both the PV panel and the refrigeration system. Further, the different control strategies where implement in these models.

2.1. Photovoltaic Modelling

The behavior of the PV-panel was modelled using a "one diode" model as described in Duffie and Beckmann (2013). The one diode model uses an equivalent circuit to describe the operation of a single solar cell. Assuming all cells to operate identically the one diode cell model can used to model a complete PV panel.
The values for the shunt and series resistances as well as the diode quality factor was determined based on standard test conditions (STC) data for a given 60 cell PV panel. The STC data may be seen in Table 1 where the assumed cell operating temperature is also stated.
As seen in Table 1 each PV panel has a STC max power output of 90 W. In order to supply sufficient power to the refrigeration systems several PV panels in parallel were applied. The present work investigated the application of both 2 and 4 PV panels in parallel, these two solutions will in the following be referred to as the 180 W and 360 W PV panels, respectively, in reference to the resulting STC maximum power output of the total installation. It should be noted that the actual maximum power of the PV panels, may be reduced as the assumed cell operating temperature of 35 °C was higher than the STC cell operating temperature.

2.2. Refrigeration System and Compressor

Table 1. Input data for the PV panel model of a single 60 cell array, operating conditions for the refrigeration system and data for the investigaed compressors

PV panel			Refrigeration system			Compressor			
Number of cells	60	-	T_{evap}	-10	°C		BD35K	BDS5.0K	
Temp. Coeff.	0.03	K^{-1}	T_{cond}	50	°C	Disp. Vol.	3	5	cm^3
STC Max Power	90	W	ΔT_{SH}	10	K	Min. Speed	2000	1000	RPM
STC Max Power Voltage	32	V	ΔT_{SC}	5	K	Max. Speed	3500	3000	RPM
STC Open Circuit Voltage	39.5	V							
STC Short Circuit Current	3	A							
Cell operating temp.	35	°C							

The modelled refrigeration system may be seen in Fig 1. Assuming a constant ambient temperature in the room where the refrigeration system was located and that the ice bank storage was kept at a constant temperature of 0 °C, it was assumed that the evaporation and condensation temperatures as well as the level of super-heating and sub-cooling would not change significantly during the operation of the system. Therefore, these values where assumed constant at the values stated in Table 1.
Two different compressors were investigated for the application in the refrigeration system, both compressors are built for R600a. The first was the BD35K which is a DC compressor produced by Nidec, the second compressor was the BDS5.0K, also produced by Nidec. The displacement volumes and speed ranges of the two compressors are stated in Table 2. As seen the BD35K has a lower displacement volume compared to the BDS5.0K and further the dynamic range of the BD35K is also significantly lower than that of the BDS5.0K.
The operational characteristics of the two compressors, i.e. isentropic and volumetric efficiencies, where modelled using speed specific compressor polynomials supplied by the manufacturer. The polynomials where supplied at four values of compressor speed ranging from the minimum to the

maximum speed. For operation at speeds in between the supplied polynomials the efficiencies where interpolated between the values of the nearest polynomials.
A part from the work derived from the application of the compressor polynomials, the initial start-up of the compressor requires additional power. This will in the following be referred to as the compressor start power. The compressor start power is associated with the initial positioning of the rotor. The start power for both compressors has been assumed to be 60 W. However, soft start procedures or the application of super capacitors may alleviate the need for the PV panel to supply the start power. Consequently, results were derived both with and without the 60 W compressor start power.

2.3. Compressor Speed Control Strategies

As the compressor in the suggested system was driven directly by the PV panel, the only manner by which sufficient utilization of the available power can be ensured was to impose a suitable compressor speed control strategy. In the present work three different speed control strategies have been investigated and compared based on their ability to utilize as much of the available power during a complete day.
To quantify to which extent the compressors utilize the available power a Utilization Factor was defined. The Utilization Factor was defined as the ratio of the integrated compressor work from sunrise to sundown over the integrated peak power over the same duration. The Utilization Factor thus indicates how well the compressor control strategy was at adapting the speed during the increasing and decreasing irradiance experienced during a day.
A part from the utilization factor the Accumulated Daily Cooling Load was also determine as the integrated cooling load delivered over the full day.
The first control strategy investigated was the PPT control. This control strategy requires the application of an external peak power tracker. The peak power tracker required the measurement of both solar irradiance and cell operating temperature which the peak power tracker then used to calculate the peak power point. This was then applied as a set point for the compressor speed regulation. Consequently, the PPT control ensured that when the compressor was on it ran at a speed at which the needed compressor power was equal to the PV panels peak power. However, the ability to run at the requested speed was limited by the minimum and maximum speeds of the compressors.
An alternative to the PPT control is CVC. As seen in Fig 2 the peak power points for increasing irradiance coincide at a close to constant voltage. Hence, it is possible to approximate the peak power point by measuring only the voltage over the PV panel. Supplying the speed control of the compressor with a set point for the PV panel voltage would thus allow the compressor to adjust the speed in order to attain a constant voltage and thus operate close to the peak power point. This control strategy alleviates the need for solar irradiance and cell temperature measurements and may thus be simpler to implement. The set point for the CVC was set to 22 V.
The final investigated control strategy was AEO. The AEO control strategy requires no additional measurements and was therefore implemented directly in the compressor, it may therefore be the most simple to implement. The principle of the AEO strategy was to continuously ramp up the compressor speed until the compressor would collapse the PV panel thus shutting the compressor off. The speed at which the collapse occurred was then stored in the controller. The compressor was then kept off for a short duration to allow pressure equalization between the condenser and

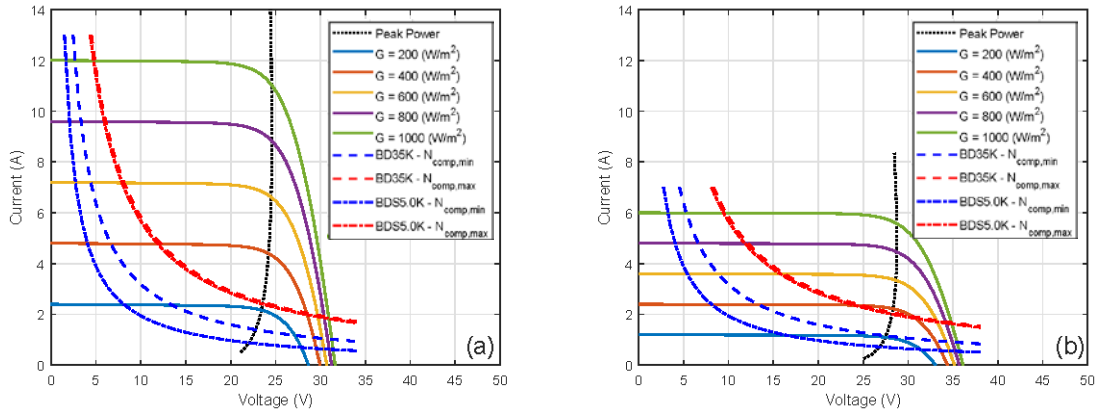

Figure 3: Current - voltage curves for the 360 W (a) and 180 W (b) PV panels, with the current - voltage curve for the two investigated compressors at their minimum and maximum compressors

evaporator in order to reduce the power consumption during start-up. It was assumed that three minutes would allow sufficient pressure equalization. After the short off-period the compressor was then turned on at a speed lower than the one at which the collapse occurred.
Two inputs are thus needed in order to run the AEO strategy, the compressor speed ramp-rate and the speed reduction when restarting the compressor. These where assumed to be constants during the operation of the system. The choice of these two constants both influence the utilization factor of the PV panel. It was found that a ramp rate of 2000 RPM $h^{-1}$and a speed reduction of 400 RPM was a good trade-off for all investigated combinations of PV panels size and compressor types.

3. RESULTS

Fig. 3 shows the voltage - current curves for the 360 W (a) and 180 W (b) PV panels, respectively. Further, the voltage - current curves for the two compressors are presented under the operating conditions shown in Table 1 and their respective minimum and maximum compressor speeds. The compressor voltage - current curves are thus iso-power lines corresponding the compressor power at minimum and maximum speeds. For a given solar irradiance the compressor must thus run between the intersections of the minimum and maximum compressor curve and the voltage - current curve at the given irradiance. If the curves do not intersect the compressor will collapse the PV panel at the minimum compressor speed and will thus not be able to run. If the PV panel voltage - current curve only intersects with the minimum speed compressor curve the compressor will be able to run at the peak power point for that irradiance and will thus be able to utilize all the available power. If the PV panel voltage - current curve intersects with both the minimum and maximum compressor speeds the compressor will not be able to run a the peak power point and will thus not be able to utilize all the available power.
This figure thus gives an indication of how well the compressor can utilize the available power from the PV panel. It may be seen that the maximum speed curves for the two compressors occurred at more or less the same point. However, the BDS5.0K could run at a lower power as the BDS5.0K had a lower minimum speed. The BDS5.0K would thus be able to run at lower levels of irradiance. Further, it may be seen that for the 360 W PV panel both compressors would not be able to run at the peak power point at irradiances much higher than 200 $Wm^{-2}$for the 180 W this was possible upto 400 Wm^{-2} However, the 180 W PV panel would require a higher irradiance before the compressor could run.

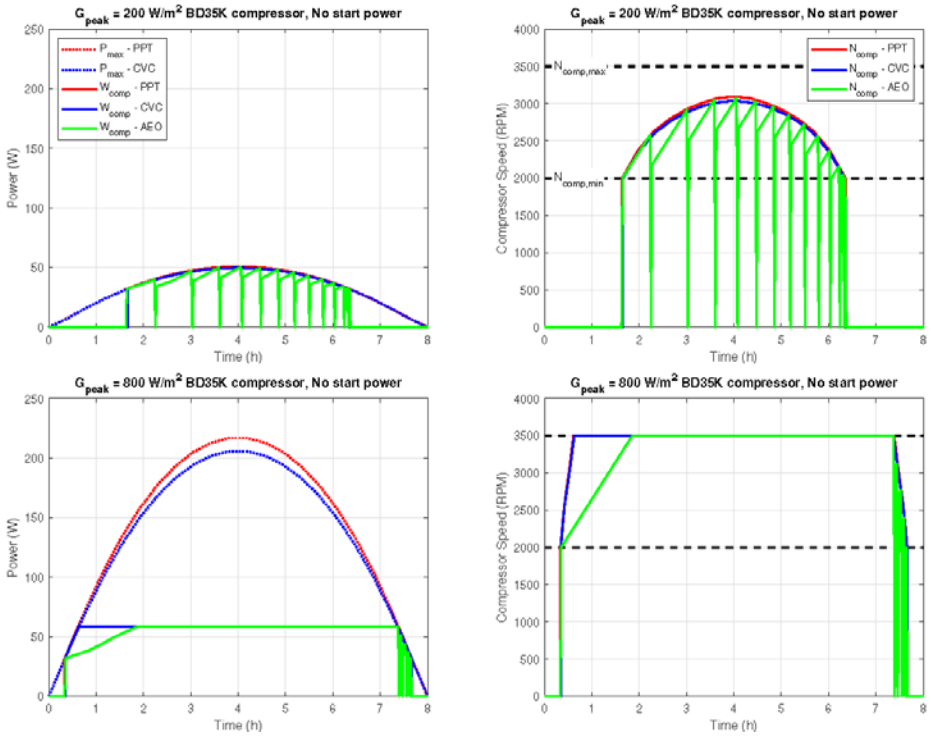

Figure 4: Compressor power and compressor speed for the PPT, CVC and AEO control strategies under two different irradiance profiles with 200 Wm^{-2} and 800 Wm^{-2} peak irradiance, respectively. Results are shown for the BD35K compressor without start power

It should be noted that the compressor start power was not included in the curves shown in Fig. 3. The need for compressor start power would shift the minimum speed curves upwards thus reducing the gap between the minimum and maximum curves.

Fig. 4 shows an example of how the different control strategies perform under two different daily profiles, with 200 $Wm^{-2}$and 800 Wm^{-2}peak irradiance, respectively. This was exemplified with the BD35K compressor without the inclusion of compressor start power and the 360 W PV panel. Fig. 4 presents both the available and utilized power and the compressor speed. As seen for both the low and the high peak irradiance profiles the three different control strategies turned the compressors on and off at more or less the same time. It may further be seen that for the 200 Wm^{-2} profile both the PPT and CVC ran at their respective maximum values while the compressors where on, further it should be noted that the difference between the PPT and CVC maximum power was insignificant. For the 200 Wm^{-2} profile the

AEO control resulted in 13 on/off cycles, however it may also been seen that the AEO actually kept the power consumption close the power consumption of the PPT and CVC control. For the 800 Wm^{-2} profile all three compressor controls strategies ran the compressors at maximum speed after 1.8 hours of sunlight, the PPT and CVC already after 0.4 hours. The compressors then ran at maximum speed until approximately 0.5 hour before sunset. The PPT and CVC subsequently reduced their speeds to the minimum before turning off 0.25 hours before sunset. In the same duration the AEO control ran 5 on/off cycles. It is clear that under the 800 Wm^{-2} peak irradiance profile non of the three control strategies would be able to utilize close the total available power.

Figs. 5 and 6 show the Utilization Factor and the Accumulated Daily Cooling Load as a function of the daily peak irradiance. This was presented for both compressors under the three compressor control strategies. Further, this was presented under four different system configuration: the 360 W PV panel and the 180 W PV panel, both with and without compressor start power.

As seen for the 360 W PV panel with 60 W of compressor start power, Figs. 5 (a) & 6 (a) the BDS5.0K compressor can deliver a cooling load as soon as the daily peak irradiance exceeds 300 Wm^{-2}, it may further be seen that the CVC control will require a slightly higher peak irradiance to run. For the BD35K the daily peak irradiance must exceed 350 Wm^{-2} to deliver a cooling load for the PPT or AEO, while the CVC again required a higher peak irradiance of about 360 Wm^{-2}.

As seen in Fig. 5 (a) the Utilization Factor increases rapidly after the minimum peak irradiance was attained and peaks shortly hereafter. Here the BDS5.0K attained the highest Utilization Factor with the PPT or CVC with a value of approximately 55 %. Here only 45 % was attained for the AEO. The

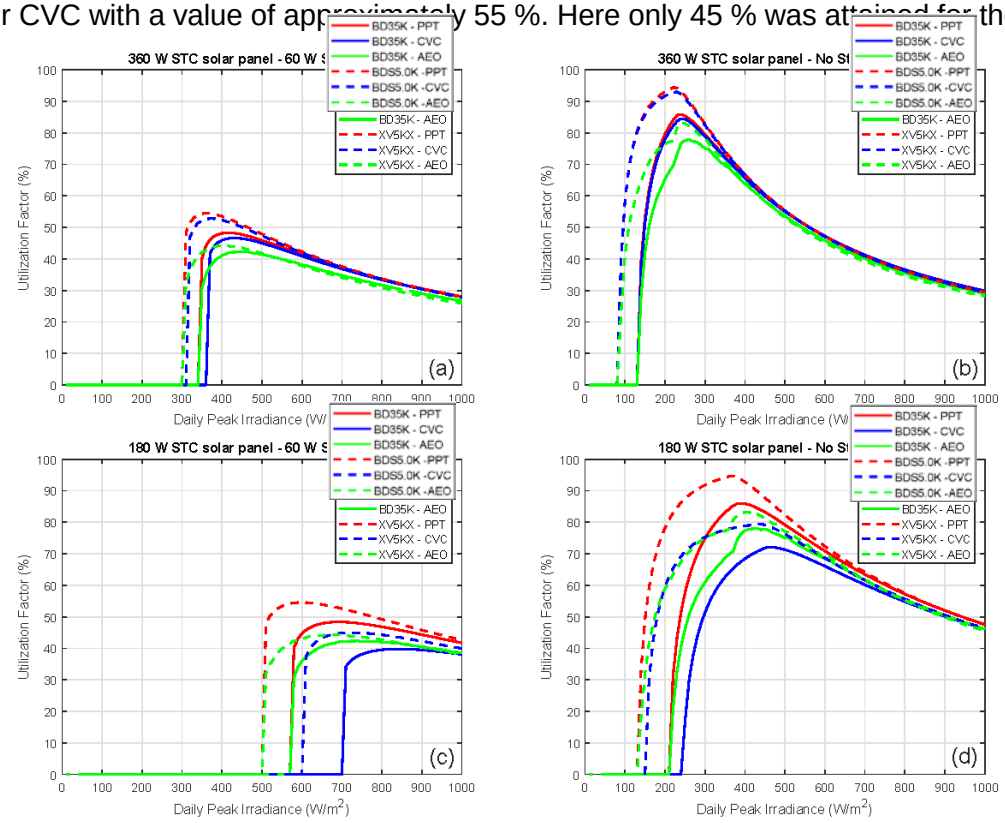

Figure 5 Compressor power and compressor speed for the PPT, CVC and AEO control strategies under two different irradiance profiles with 200 Wm^{-2} and 800 Wm^{-2} peak irradiance, respectively. Results are shown for the BD35K compressor without start power

BD35K utilized less of the available power, peaking at around 48 % for the PPT and CVC and around 42 % for the AEO. As the daily peak irradiance increases the differences between the Utilization Factor of the two compressors and the different control strategies diminished and at a daily peak irradiance of a 1000 Wm^{-2} the Utilization Factor was approximately 28 % for all six options.
As seen in Fig. 6 (a), then although there was only a minor difference between the Utilization Factor of the two compressors, the Accumulated Daily Cooling Load differs significantly. Here the BDS5.0K was capable of delivering more cooling load than the BD35K, as the BDS5.0K compressor was more efficient. Again it may be seen that the PPT and CVC attain comparable cooling loads while the AEO delivered slightly less.
Assuming that the need for compressor start power can be alleviated but keeping the PV panel size of 360 W results in the Utilization Factor and Accumulated Daily Cooling Loads seen in Figs. 5 (b) & 6 (b). As seen this allowed the compressors to run at significantly lower daily peak irradiances. Here the all three strategies delivered a cooling load already from a daily peak irradiances of 90 W for the BDS5.0K and 120 W for the BD35K. Again the Utilization Factors show a rapid increase as soon as the minimum irradiance was attained. Here the BDS5.0K with the PPT and CVC peaks at a Utilization Factor of 94 % while the AEO reached around 83 %. The BD35K again utilized less of the available power peaking at around 84 % for the PPT and CVC and 78 % for the AEO. Again the differences between the utilization Factors of the two compressors and the three control strategies diminishes with increasing peak irradiance reaching approximately 30 % with a peak irradiance of 1000 Wm^{-2}. As shown previously, the BDS5.0K delivers significantly more cooling load than the BD35K, see 6 (b). As was also shown earlier the AEO delivers less cooling load compared to the CVC and PPT, however when the need for start power was alleviated the AEO approaches the load delivered by the CVC and PPT.
When the PV panel size was reduced to 180 W while still supplying the 60 W of start power, the minimum peak irradiance increases significantly, see Figs. 5 (c) and 6 (c). As seen the BDS5.0K with either the PPT or AEO requires a peak irradiance in excess of 500 Wm^{-2}, while the CVC requires 600 Wm^{-2}.For the BD35K this was 590 Wm^{-2} for the PPT and AEO and 700 Wm^{-2} for the CVC. In light of these results, this configuration was deemed infeasible as it would result in the lack of cooling load for too many days.

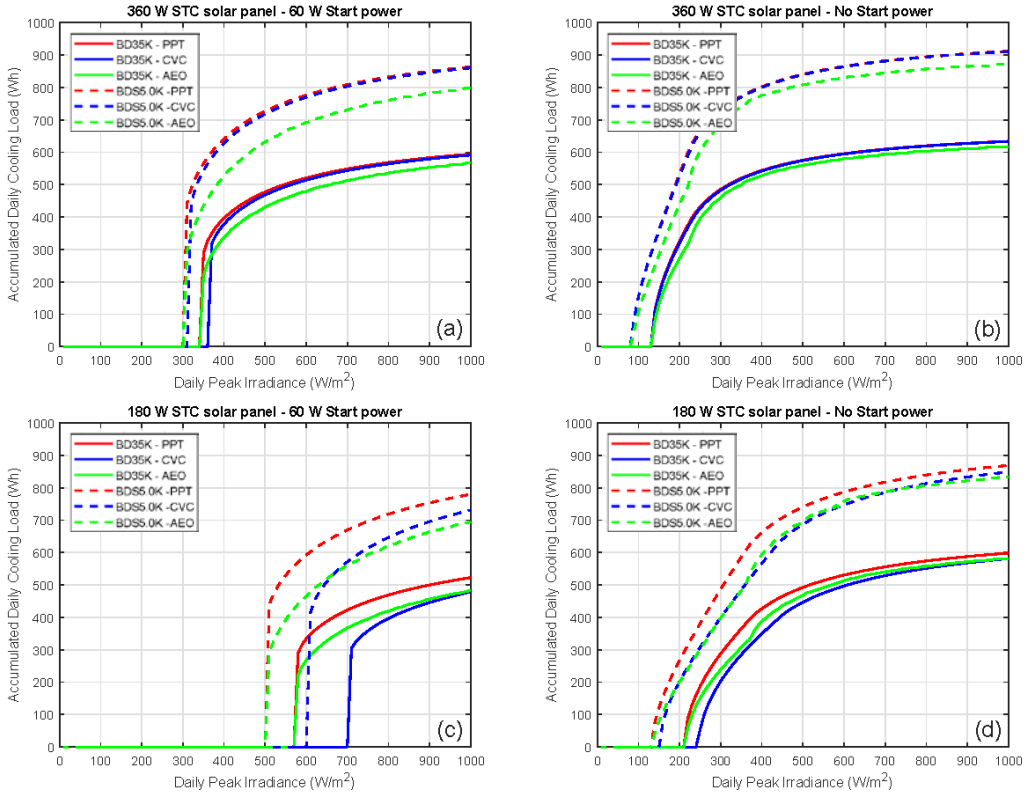

Figure 6: Daily accumulated cooling for the BD35K and BDS5.0K compressors under the PPT, CVC and AEO control strategies using both the 180 W and 360 W PV panels and with and without compressor start power delivered from the PV panel

However, if the need for compressor start power was alleviated for the 180 W panel the minimum peak irradiance was again significantly reduced, see Figs. 5 (d) and 6 (d). Here the BDS5.0K will be able to deliver a cooling load from around 120 Wm^{-2} while the BD35K would require slightly more than 200 Wm^{-2}. Generally, it may be seen that the Utilization Factor for this configuration was higher than the remaining configurations. Even at 1000 Wm^{-2} almost 50 % of the available power was utilized. As seen the Accumulated Daily Cooling Load was actually comparable to that of the 360 W with 60 W start power when both are running. As such it can be concluded that if the compressor start power can be alleviated the PV panel size can be halved without reducing the delivered cooling load, actually the cooling load can be delivered at lower irradiances with half the PV panels if start power was avoided. Finally, it may seen that for this configuration there was slightly higher difference between the applied control strategy.

4. CONCLUSIONS

The influence of compressor type and compressor control strategy on the performance of a solar direct drive refrigeration system was investigated using numerical modelling and simulations. The Utilization Factor and Accumulated Daily Cooling Load were determined for a full day under varying daily peak irradiances. Two compressor types, the BDS5.0K and BD35K and three compressor control strategies, PPT, CVC and AEO where investigated. Further, four configuration where included: a 360 W and a 180 W PV panel both with and without compressor start power delivered from the PV panel. Results showed that both the choice of compressor and the applied control strategy affected the systems ability to utilize the available power from the PV panel, especially under lower irradiance conditions and when the PV panel was downsized. Generally, the PPT strategy delivered the highest Utilization Factor and thus the highest cooling load. The CVC was comparable to the PPT for the 360 W PV panel, while performing worse than the PPT for the 180 W configurations. The AEO generally had a lower performance than the PPT and CVC. However, compared to the simplicity of this control strategy the AEO actually performed well compared to the more challenging PPT and CVC controls. The BDS5.0K performed better than the BD35K due to both the increased efficiency and the increased speed range. Finally, results show that if the need for compressor start power delivered by the PV panel was alleviated the size of the PV panel can be halved without a significant reduction in performance.

ACKNOWLEDGEMENTS

This research project is financially funded by EUDP (Energy Technology Development and Demonstration). Project title: "Second Generation Solar Direct Drive Refrigerators", project number: 64017-0556

REFERENCES

Duffie, J.A., Beckmann, W.A., 2013. Solar Engineering of Thermal Processes. John Wiley and Sons, New Jersey.

IEA, 2012. Measuring progress towards energy for all: power to the people? World energy outlook, Organisation for Economic Co-operation and Development, Paris, France.

McCarney, S., Robertson, J., Arnaud, J., Lorenson, K., Lloyd, J., 2013. Using solar-powered refrigeration for vaccine storage where other sources of reliable electricity are inadequate or costly. Vaccine 31, 6050–6057. doi:10.1016/j.vaccine.2013.07.076.

Myers, D., Diesburg, S., Lennon, P., McCarney, S., 2017. Energy harvesting controls for solar direct drive medical cold chain equipment. Ghtc 2017 - Ieee Global Humanitarian Technology Conference, Proceedings 2017-, 1–9. doi:10.1109/GHTC.2017.8239228.

Pedersen, P.H., Katic, I., Markussen, W.B., Jensen, J.K., Cording, C., Moeller, H., 2019. Direct drive solar coolers. The 25th IIR International Congress of Refrigeration, August 24-30, Montreal, Canada doi:10.18462/iir.icr.2019.